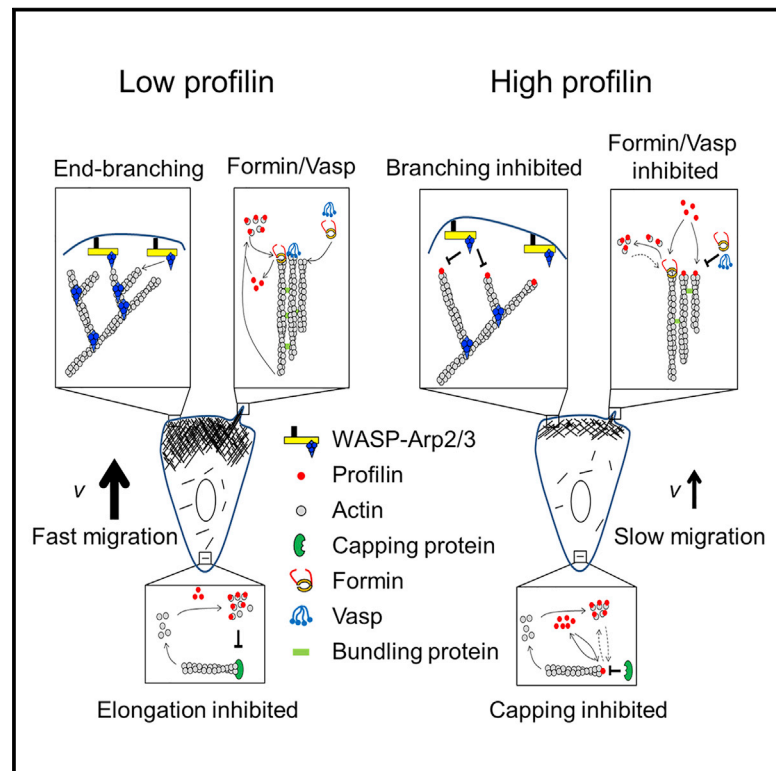


Developmental Cell

Profilin Interaction with Actin Filament Barbed End Controls Dynamic Instability, Capping, Branching, and Motility

Graphical Abstract



Authors

Julien Pernier, Shashank Shekhar, Antoine Jegou, Bérengère Guichard, Marie-France Carlier

Correspondence

marie-france.carlier@i2bc.paris-saclay.fr

In Brief

Pernier et al. demonstrate how the binding of profilin to actin filament barbed ends affects actin homeostasis during cell migration. Profilin competes with and coordinates the function of barbed end regulators including Capping Protein, polymerases such as formin or VASP, and WASP-Arp2/3 filament branching machineries.

Highlights

- The binding of profilin to barbed ends accounts for its effects on cell migration
- Profilin enhances length fluctuations of actin filaments by destabilizing barbed ends
- Profilin competes with capping protein at filament barbed ends
- Profilin competes with polymerases and filament branching machineries at barbed ends



Profilin Interaction with Actin Filament Barbed End Controls Dynamic Instability, Capping, Branching, and Motility

Julien Pernier,^{1,2} Shashank Shekhar,^{1,2} Antoine Jegou,^{1,3} Bérengère Guichard,^{1,3} and Marie-France Carlier^{1,*}

¹Cytoskeleton Dynamics and Motility Group, I2BC, CNRS, Gif-sur-Yvette 91198, France

²Co-first author

³Present address: Regulation of Actin Assembly Dynamics Group, Institut Jacques Monod, Université Paris-Diderot, Paris 75205, France

*Correspondence: marie-france.carlier@i2bc.paris-saclay.fr

<http://dx.doi.org/10.1016/j.devcel.2015.12.024>

This is an open access article under the CC BY-NC-ND license (<http://creativecommons.org/licenses/by-nc-nd/4.0/>).

SUMMARY

Cell motility and actin homeostasis depend on the control of polarized growth of actin filaments. Profilin, an abundant regulator of actin dynamics, supports filament assembly at barbed ends by binding G-actin. Here, we demonstrate how, by binding and destabilizing filament barbed ends at physiological concentrations, profilin also controls motility, cell migration, and actin homeostasis. Profilin enhances filament length fluctuations. Profilin competes with Capping Protein at barbed ends, which generates a lower amount of profilin-actin than expected if barbed ends were tightly capped. Profilin competes with barbed end polymerases, such as formins and VopF, and inhibits filament branching by WASP-Arp2/3 complex by competition for filament barbed ends, accounting for its as-yet-unknown effects on motility and metastatic cell migration observed in this concentration range. In conclusion, profilin is a major coordinator of polarized growth of actin filaments, controlled by competition between barbed end cappers, trackers, destabilizers, and filament branching machineries.

INTRODUCTION

Motile and morphogenetic processes are driven by polarized assembly of actin filaments, which generates protrusive or compressive forces against cellular membranes. Filament growth rate is controlled by the concentration of polymerizable monomeric actin that associates to barbed ends and by the activity of regulatory proteins at barbed ends (Carlier et al., 2015). Profilin, an essential actin-binding protein present in cells in the range 10–80 μM (dos Remedios et al., 2003; Witke et al., 2001), is a central player in actin-based motility, because profilin-actin complex feeds filament assembly selectively at barbed ends (Pollard and Cooper, 1984) and supports formin-mediated rapid processive barbed end assembly (Kovar et al., 2003; Romero et al., 2004). Thus, like free G-actin, profilin-actin is in dynamic equilibrium

with F-actin at barbed ends. This is in contrast with β -thymosin, which forms non-polymerizing complexes with actin that are in rapid equilibrium with G-actin but not with F-actin.

While the cellular function of profilin is thought to be linked to its binding G-actin, elusive effects of profilin in motile and metastatic processes cannot easily be explained within this simple view. Injection of profilin inhibits lamellipodium motility and formation of the lamellipodial branched filaments (Cao et al., 1992; Rotty et al., 2015; Suarez et al., 2015). Consistently, profilin is downregulated in invasive metastatic breast cancer cells (Joy et al., 2014; Lorente et al., 2014) and its overexpression reduces their migration (Roy and Jacobson, 2004). These counterintuitive facts prompted us to take a new look at profilin.

Profilin associates with the barbed face of actin, which is exposed on both G-actin and F-actin at the filament barbed end. Profilin binds G-actin with high affinity ($K_G = 0.1 \mu\text{M}$), and barbed end F-actin with relatively lower affinity ($K_F = 20 \mu\text{M}$), promoting enhanced filament disassembly (Bubb et al., 2003; Courtemanche and Pollard, 2013; Jegou et al., 2011; Kinosian et al., 2002). The consequences of profilin's interaction with barbed ends on filament assembly dynamics and profilin's resulting competition with other barbed end regulators are explored here.

We find that profilin enhances fluctuations in the length of filaments. The extensive disassembly events are balanced by an increased amount of profilin-actin feeding barbed ends at steady state. We next reveal that profilin controls actin homeostasis by competing with Capping Protein (CP) at barbed ends, with formin and with WH2-domain-containing barbed end trackers such as VopF. Finally, profilin binding to barbed ends inhibits filament branching by WASP proteins and Arp2/3 complex and resulting actin-based motility. Proteins that track barbed ends such as VopF, VASP, formins, similarly inhibit filament barbed end branching by Arp2/3 complex. The reported “anti-capping” and “anti-branching” activities of profilin, which affect motility, are explained by competitive interplay of regulators at barbed ends.

RESULTS

Profilin Enhances Length Fluctuations of Actin Filaments in ATP

Actin filaments, like microtubules, use nucleotide hydrolysis associated with assembly to generate metastable dynamic polymers. Rapid disassembly of the ADP/GDP subunits in the core of

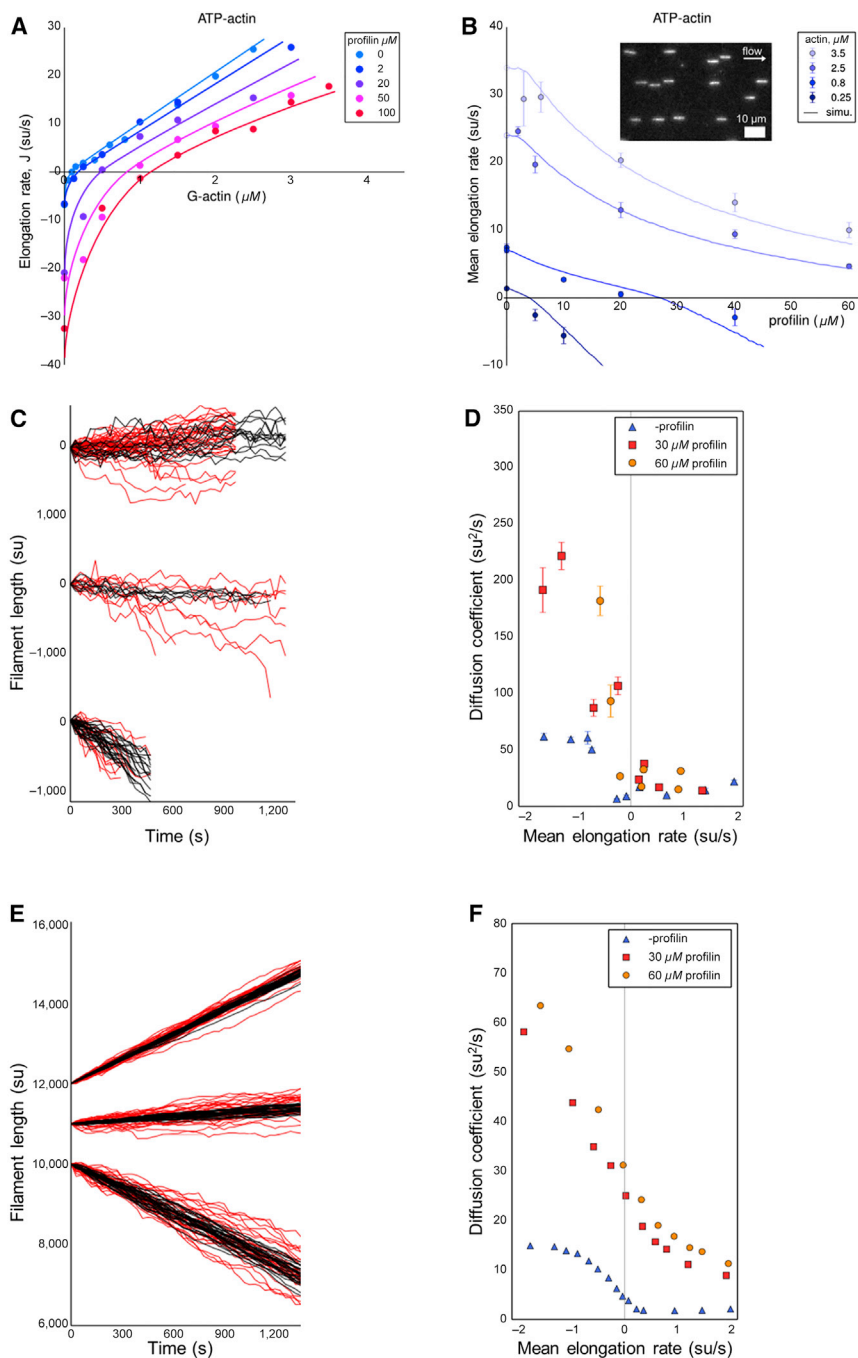


Figure 1. Profilin Promotes Mild Dynamic Instability of Actin Filaments

(A) Effect of profilin on the rate of barbed end growth as a function of MgATP-G-actin, monitored using the pyrene fluorescence assay. See [Supplemental Experimental Procedures](#) for details.

(B) Effect of profilin on the rate of barbed end growth of single filaments initiated from immobilized spectrin-actin seeds (open symbols). Lines: numerical simulations, using the kinetic parameters in [Table S1](#). Inset: individual filaments observed in microfluidics-assisted microscopy.

(C and E) Length of individual filaments versus time, without (black) or with (red) 30 μM profilin were measured (C) or simulated numerically (E) with the same parameters as in [Figure 1B](#). Actin concentrations are adjusted to obtain mean elongation rates of -1.6 , -0.25 , and 0.8 subunits/s (C) and -2 , 0.3 and 2 subunits/s (E). Curves are shifted vertically for readability.

(D and F) 1D diffusion coefficient D , from experimental (D) or numerical (F) data, for mean growth rates around null (vertical gray line) with or without profilin as indicated. Error bars are SDs.

centration C_{SS} at which the net rate of filament barbed end growth is null, we first examined how the rate of barbed end elongation, J , at varied G-actin concentrations (C) is affected by profilin ([Figure 1A](#)). Only barbed ends contribute in $J(C)$ since pointed ends do not interact with profilin and disassemble extremely slowly. The dual activity of profilin is revealed by the data. In a range of profilin concentrations sufficient to convert G-actin into profilin-actin, barbed end growth proceeds equally well from profilin-actin or G-actin. At a range of higher concentrations (10–100 μM), profilin-enhanced dissociation from barbed ends promotes an increase in C_{SS} ($J(C_{SS}) = 0$) from 0.1 μM up to 1 μM at 50 μM profilin, and 1.3 μM profilin-actin at 100 μM profilin. This means that an enhanced flux of profilin-actin association to barbed ends balances enhanced disassembly at steady state. The increase in C_{SS} is the signature of the destabilization of filament barbed

the polymer is prevented by a stable ATP/GTP cap at the growing plus/barbed end ([Carlier et al., 1984](#)). Dynamic instability is milder in actin than in microtubules ([Hill, 1986](#); [Ranjith et al., 2009](#); [Stukalin and Kolomeisky, 2006](#); [Vavylonis et al., 2005](#)). Yet, fluctuations in the length of individual filaments, exceeding the low “length diffusivity” of reversible polymerization, have been detected ([Fujiwara et al., 2002](#); [Kuhn and Pollard, 2005](#)).

Profilin was predicted to enhance length fluctuations by promoting faster filament disassembly ([Jegou et al., 2011](#)). To measure length fluctuations in the region of the monomer con-

ends by profilin. In measurements of F-actin at steady state described later ([Figures 4C, 4D, and 5E](#)), the same values of C_{SS} are found for profilin-actin co-existing at steady state with F-actin.

Single-filament kinetics using microfluidics-assisted microscopy of filaments immobilized at their pointed ends by spectrin-actin seeds confirmed the destabilization of barbed ends by profilin seen in bulk solution measurements ([Figure 1B](#), symbols). Computed rates of filament growth using parameters for profilin binding to ATP-bound barbed ends ([Table S1](#)) confirm the experimental data ([Figure 1B](#)).

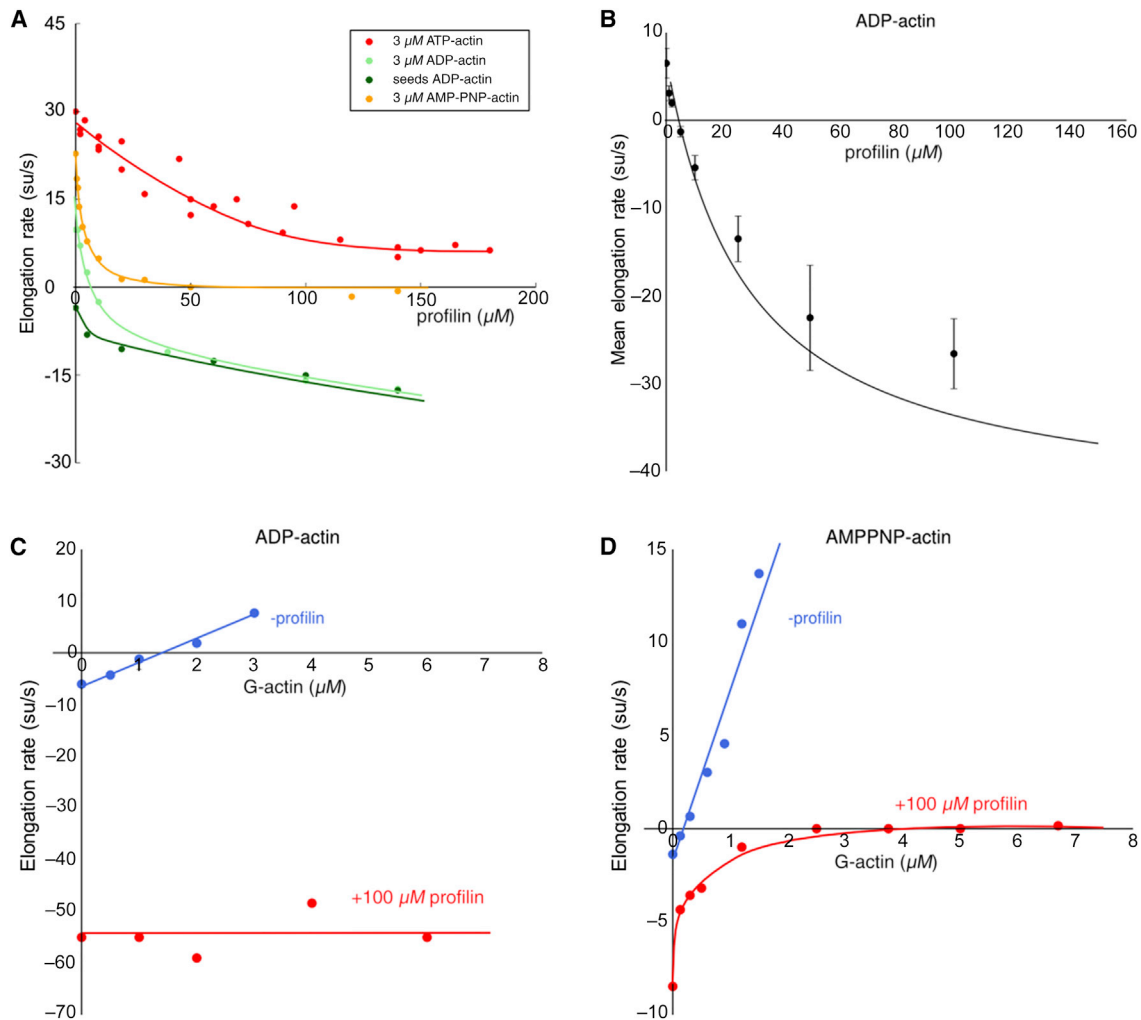


Figure 2. Nucleotide Dependence of the Effect of Profilin

(A) Effect of profilin on the rate of filament elongation in ATP, AMPPNP, and ADP. Conditions as in Figure 1A, with 3 μM G-actin. Dark green curve: in ADP, no G-actin.

(B) Single filament experiments at 5 μM ADP-actin. Data points from Jegou et al. (2011). The solid line is computed using parameters from Table S1, assuming that the barbed end on-rate constant for profilin-ADP-actin is the same as for ADP-actin ($2.6 \mu\text{M}^{-1} \text{s}^{-1}$). Error bars are standard deviations.

(C) Effect of profilin on barbed end assembly in ADP (C) and AMPPNP (D). Blue curves, no profilin; red curves, 100 μM profilin.

We then compared fluctuations in length in the absence and presence of free profilin in the vicinity of C_{SS} (from Figures 1A and 1B) at a range of growth rates of -2 to $+2$ subunits/s (Figures 1C and 1D). The diffusion coefficient D was 10 ± 2 subunits²/s for non-capped filaments at steady state in the absence of profilin, one order of magnitude higher than for capped filaments (0.31 ± 0.2 subunits²/s, the detection limit). Over a wide range of elongation rates, fluctuations are enhanced by profilin, most extensively below C_{SS} , as predicted (Vavylonis et al., 2005), where the maximal value of D was increased up to 5-fold at 30 μM profilin (Figure 2B). These features are reproduced in simulated kinetics of growth of individual filaments (Figures 1E and 1F), using the same parameters as in Figure 1B (Table S1; see Supplemental Experimental Procedures, Equation 1).

In conclusion, profilin promotes a mild form of “dynamic instability” in actin, by amplifying the effects of catastrophes above

the critical concentration, and of rescues below the critical concentration. The filament monomer-polymer exchanges are largely dominated by profilin-actin exchanges at barbed ends exclusively.

Effect of Profilin on Barbed End Assembly from ATP-, ADP-, and AMPPNP-Actin

Profilin affects barbed end assembly differently depending on the nature of the actin-bound nucleotide (Figure 2A). While profilin slowed down barbed end assembly at 3 μM ATP-G-actin, consistent with the results in Figure 1A, it inhibited assembly at 3 μM ADP-G-actin, eventually causing barbed end disassembly at the same rate as in the absence of actin. Thus, filaments are unable to elongate from profilin-ADP-actin. This was confirmed in single-filament assays (Figure 2B). Finally, profilin inhibited filament growth from AMPPNP-actin. However, the barbed

ends remained blocked by profilin-AMPPNP-actin and no depolymerization of AMPPNP-F-actin was observed at high profilin.

In the absence of profilin, J(C) plots obtained in ADP and AMPPNP were linear as expected, with critical concentration values of 1.5 μM and 0.14 μM , respectively (Figures 2C and 2D). In the presence of 100 μM profilin, ADP-F-actin depolymerized at a high rate (55 subunits/s) independent of ADP-G-actin, consistent with Figure 2A. In contrast, AMPPNP-F-actin depolymerized at a 10-fold enhanced rate in the absence of actin, in agreement with Courtemanche and Pollard (2013), but the addition of AMPPNP-G-actin gradually led to total blockage of barbed ends, consistent with Figure 2A. In conclusion, profilin binds G-actin and barbed ends in various bound nucleotide states, but only profilin-MgATP-actin supports barbed end assembly.

Capping Protein and Profilin Compete at Filament Barbed Ends: Implication in the Control of the F-Actin/G-Actin Ratio and Free Profilin Concentration

In live cells, most profilin is thought to be bound to G-actin (Kaiser et al., 1999). This view is based on the implicit assumption that barbed ends are fully capped in the bulk cytoplasm, which prevents the participation of profilin-actin in barbed end growth. In these conditions, profilin is now in equilibrium with G-actin only at the critical concentration for pointed end assembly, leading to 88% of total profilin being present in profilin-actin complex (Equation 2, Supplemental Experimental Procedures). Typically, in a cell containing 50 μM profilin, 43 μM profilin-actin would be present (Sirotkin et al., 2010), which would support transient barbed end growth of newly formed filaments at a rate of 1 $\mu\text{m/s}$, and formin-bound barbed ends at 5–10 $\mu\text{m/s}$. These rates are much higher than those observed so far, which suggests that the amount of profilin-actin is lower than predicted by strong capping.

How does the interaction of profilin with barbed ends interfere with the function of CP, the most ubiquitous and abundant barbed end capper? CP is required in motile processes such as lamellipodia (Edwards et al., 2014). CP binds terminal actin subunits with a K_d of 0.1 nM (Wear et al., 2003). Tuning the extent of barbed end capping in the cytoplasm is essential. Over 90% of filaments must be capped to maintain a high concentration of actin monomers available for transient localized barbed end assembly in motility (Carlier and Pantaloni, 1997; Hug et al., 1995; Walsh et al., 1984). However, capping of 100% barbed ends inhibits all actin-based movements. Clearly, the potential competition between profilin and CP and its consequences in motility have to be addressed.

Binding of CP (1 nM) to the growing barbed ends of single filaments was slowed down by profilin (Figure 3A), consistent with profilin binding to terminal ATP-F-actin ($K_F = 29.3 \pm 1.7 \mu\text{M}$), in competition with CP (Table S1). Similarly, profilin slowed down binding of CP in ADP-F-actin depolymerization assays (Figure S1A). In contrast, depolymerization of CP-capped filaments was unaffected by up to 100 μM profilin (Figure S1B). Hence, profilin inhibits CP association to barbed ends but does not uncap CP from barbed ends, in agreement with Bubb et al. (2003). These effects are observed in a physiologically relevant range of concentrations of profilin (dos Remedios et al., 2003) and of free CP, since the major fraction

of cellular CP (total concentration 1–2 μM) is sequestered by myotrophin/V1 (see Discussion).

How does the competition between profilin and CP affect the distribution of the filament population between the capped (blocked) and non-capped (dynamic) state? To address this issue, we measured the steady state amount of F-actin at different concentrations of CP and profilin in the range 0–10 μM (Figures 3B and S1C). In the absence of profilin, CP caused partial depolymerization of 0.5 μM F-actin, corresponding to the increase in the critical concentration from 0.1 to 0.6 μM , its value for pointed end assembly (Figure 3B inset, blue symbols). The major change in critical concentration (Walsh et al., 1984) occurs between 90% capping (1 nM CP) and 99% capping (10 nM CP). Addition of increasing amounts of profilin to filaments containing between 10 and 100 nM CP did not promote a linear decrease in F-actin leading to complete disassembly, as observed when barbed ends are strongly capped by gelsolin (orange triangles in Figure 3B; Equation 2, Supplemental Experimental Procedures). Strikingly, only partial F-actin disassembly was recorded (Figures 3B and S1C). A stationary level of profilin-actin, which increased with CP, was established at 10 μM profilin in dynamic equilibrium with the remaining F-actin (Figure 3B inset, red symbols). In conclusion, by antagonizing capping of barbed ends by CP, profilin maintains active monomer-polymer exchange at a fraction of barbed ends. The thermodynamic data thus agree with the kinetic data.

These results were corroborated by sedimentation assays. SDS-PAGE analysis and pyrenyl-fluorescence measurements of profilin-actin in the supernatants of F-actin (20 μM) capped by either CP or gelsolin, (Figure 3C) confirm that profilin (50 μM) promotes complete depolymerization of gelsolin-capped filaments but only partial depolymerization in the presence of CP, leaving 80% profilin free.

To confirm that the difference in behavior of profilin with CP-capped and gelsolin-capped filaments results specifically from its ability to interact with barbed ends, we used thymosin β_4 as a passive G-actin sequesterer that does not interact with actin filaments. In contrast with profilin, thymosin β_4 caused identical depolymerization of F-actin when filaments were capped by either CP or gelsolin (Figure 3D).

In conclusion, the ability of profilin to compete with CP lowers the fraction of profilin in the actin-bound state and imposes a higher amount of free profilin than expected in conventional views. Free profilin can thus compete effectively with other barbed end binding proteins. A diagram summarizing the distributions of F-actin, free profilin, and profilin-actin in various states of barbed ends and at physiologically relevant concentrations of all proteins is shown as an illustration (Figure 3E).

Profilin Competes with Barbed End Tracking Proteins and Formin

How does profilin also compete with polymerases that track barbed ends? Potential candidates include formins (Goode and Eck, 2007) and multimeric WH2 domain proteins such as VopF and VASP (Breitsprecher et al., 2008; Hansen and Mullins, 2010; Pernier et al., 2013). The FH2 domain of formins and the WH2 domains display steric clashes with profilin binding to the barbed face of terminal F-actin (Carlier et al., 2015). On the other hand, association of profilin-actin to the FH1 domain of formin is

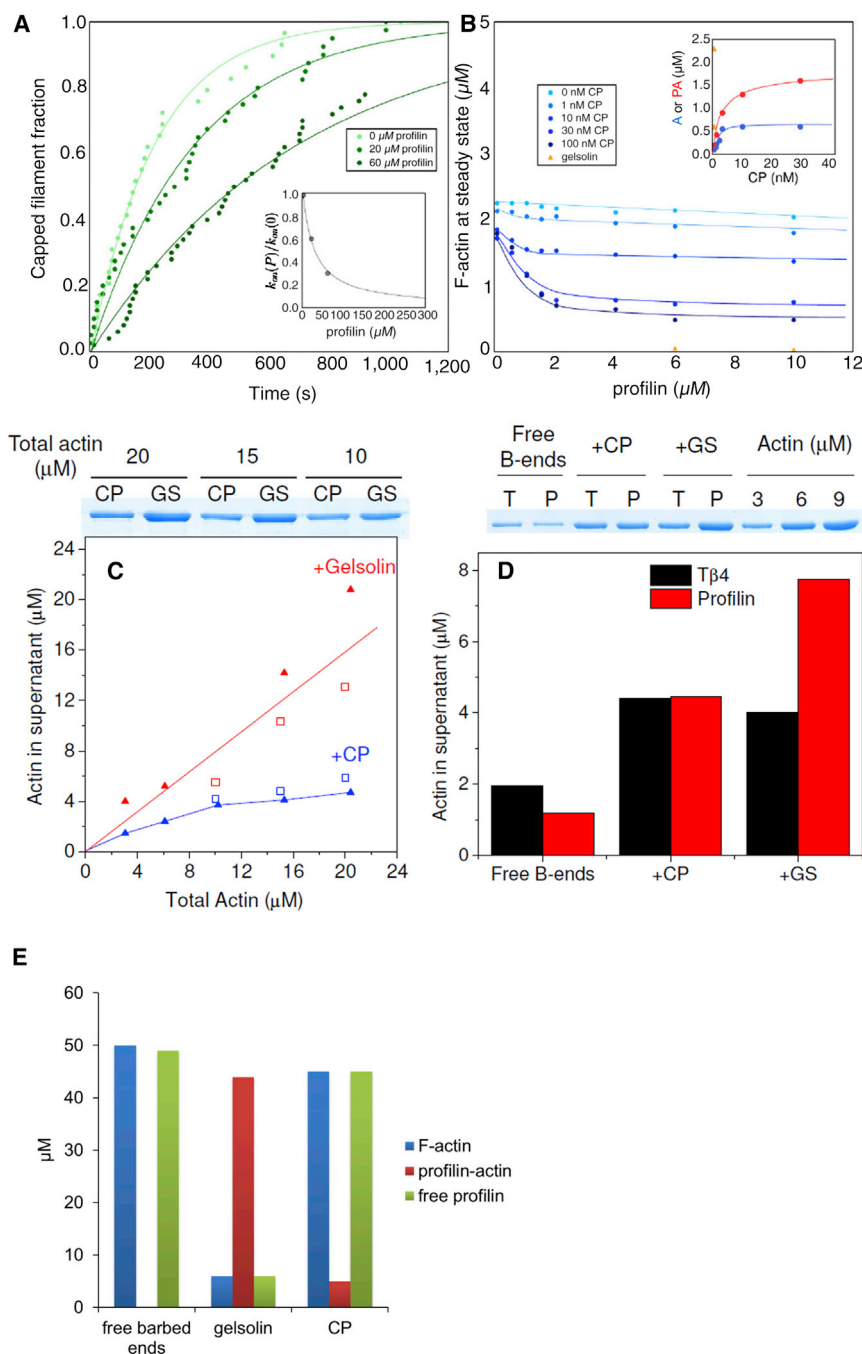


Figure 3. Profilin Competes with CP at Barbed Ends

(A) Time course of the fraction of individual filaments that get capped for the first time, in the presence of 1 nM CP and 0, 20, or 60 μM profilin, and G-actin at concentrations ensuring a growth rate of 10 subunits/s (see [Supplemental Experimental Procedures](#)). Inset: Pseudo first-order rate constant for CP binding versus profilin, representing binding of profilin to ATP-bound barbed ends ($K_d = 29.25 \pm 1.75 \mu\text{M}$).

(B) F-actin assembled at steady state (2.3 μM F-actin, 2% pyrenyl labeled) in the absence and the presence of CP, and profilin as indicated. Inset: concentration of actin monomers at steady state versus CP, in the absence (blue sigmoidal curve) or the presence of 5 μM profilin (red curve). Data derived from main frame. Orange triangles, gelsolin in place of CP.

(C) Profilin-actin complex in the supernatants of F-actin assembled at 20 μM in the presence of either 100 nM CP (blue symbols) or gelsolin at a 1:300 ratio to actin (red symbols). Closed and open symbols represent values derived from pyrene fluorescence and SDS-PAGE (top panel), respectively.

(D) Unassembled actin in supernatants of F-actin assembled in the presence of thymosin $\beta 4$ or profilin, and CP or gelsolin. Note that in contrast to profilin, thymosin $\beta 4$ sequesters actin identically when filaments are capped by CP or by gelsolin. Top panel: SDS-PAGE of the samples.

(E) Distribution of F-actin, profilin-actin, and free profilin in a medium containing 50 μM total actin and 50 μM total profilin, with various states of barbed ends.

essential for rapid processive assembly by formins (Kovar et al., 2006; Romero et al., 2004). Thus, the effects of profilin on formin function are potentially complex. Excess of free profilin inhibits processive elongation of filaments by formin (Kovar et al., 2006). Profilin also inhibits FH2 (Higgs, 2005; Scott et al., 2011). Thus, inhibition of formin by profilin may not be due only to displacement of profilin-actin from the FH1 domain.

How profilin affects the kinetics of FH1-FH2 of mDia1 association to barbed ends was addressed in microfluidics-assisted total internal reflection fluorescence (TIRF) microscopy assays (Figure 4A). The free barbed end of spectrin-actin initiated fila-

ments was exposed briefly to FH1-FH2 in the presence of varying concentrations of profilin, before being exposed to profilin-actin only. Free and formin-bound barbed ends were discriminated by their rate of barbed end growth in profilin-actin (Figure S2A). Profilin inhibited binding of formin to barbed ends in a saturation fashion, consistent with a mutually exclusive binding scheme and a binding constant of profilin of 34 μM for barbed ends. The effect of profilin on the kinetics of processive assembly was analyzed. Whether formin was (Figure S2B) or was not anchored (Figure 4B), a bell-shaped dependence of the rate of processive assembly on profilin was observed. Effective processive depolymerization was observed at high profilin. In the absence of actin, profilin enhanced depolymerization of FH1-FH2 bound filaments, in agreement with data obtained with anchored formin (Jegou et al., 2013). Controls run in comparison with free barbed ends are shown. Together, the data demonstrate that profilin destabilizes the barbed ends without displacing FH1-FH2. Remarkably, while formin “protects” barbed ends from destabilization by profilin in the presence of actin, it amplifies profilin-induced destabilization in the absence of actin.

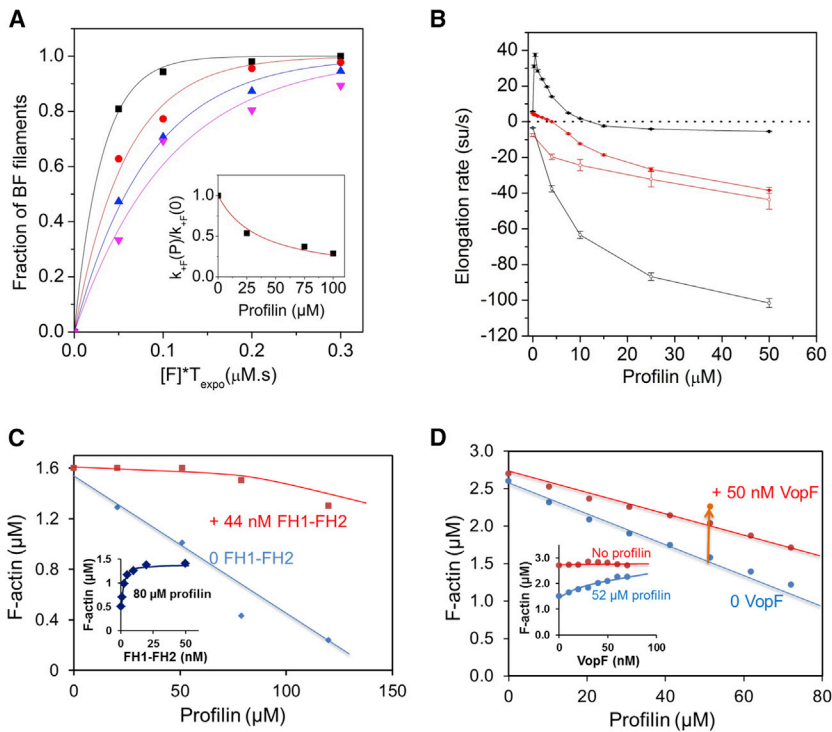


Figure 4. Competition between Profilin and Formin or VopF for Barbed Ends

(A) Profilin inhibits FH1-FH2 association to barbed ends: Filaments elongated from coverslip-immobilized spectrin-actin seeds and exposing free barbed ends (B) were first incubated with 10 nM FH1-FH2 (F) and 0 μM (black), 25 μM (red), 75 μM (blue), or 100 μM profilin (magenta) (and no actin) for various periods of time (Figure S2A), then immediately exposed to a flow of profilin-actin. The fraction of filaments in BF (fast growth) and B (slow growth) states was measured (Shekhar et al., 2015). Symbols: data points for 5, 10, 20, and 30 s exposure time. Lines: exponential fits. Inset: Pseudo first-order rate constant for formin binding versus profilin, representing the saturation of ATP-bound barbed ends by profilin ($K_d = 36.52 \pm 4.1 \mu\text{M}$). At least 150 filaments were observed for each combination of exposure time and profilin concentration.

(B) Profilin first assists, then inhibits formin-based rapid elongation at high profilin concentration. Filaments initiated from immobilized spectrin-actin seeds with free (red) or formin-bound (black) barbed ends are exposed to a flow containing profilin only (open symbols) or profilin with 0.5 μM G-actin (closed symbols). Barbed end elongation rates are monitored, $N = 40\text{--}50$ filaments. Error bars are SEM.

(C) Profilin and formin antagonize in controlling the steady-state of actin assembly. Amount of F-actin

at steady state (2 μM actin) as a function of profilin in the absence and the presence of 44 nM FH1-FH2. Inset: effect of FH1-FH2 on F-actin at 80 μM profilin. (D) Profilin and VopF antagonize in controlling the steady-state of actin assembly. Amount of F-actin at steady state in the absence and the presence of VopF (red, 50 nM; orange, 70 nM) and profilin. Inset: Effect of VopF on F-actin at 52 μM profilin.

The above kinetic data are confirmed by the thermodynamic data. Formin, VopF, and VASP all maintain a low critical concentration (high stability) of barbed ends (Pernier et al., 2013; Romero et al., 2004). Here we show that formin (Figure 4C) as well as VopF (Figure 4D) similarly antagonize the destabilizing effect of profilin at barbed ends by increasing the amount of F-actin (Experimental Procedures). The general view that reactivity of barbed ends is controlled by competitive binding is not new. VopF uncaps CP from barbed ends using its WH2 domains, the dissociation of CP being enhanced by VopF via a transient low-affinity ternary complex with barbed ends (Pernier et al., 2013). Formin uncaps CP using the same molecular mechanism (Shekhar et al., 2015).

Profilin Binding to Barbed Ends Inhibits Filament Branching by N-WASP with Arp2/3 Complex and Actin-Based Motility

The intriguing effects of profilin on cell motility reported earlier cannot be explained merely by its competition with barbed end trackers. In particular, the selective inhibition of lamellipodium (Cao et al., 1992), the disappearance of the WAVE-Arp2/3 branched filament array at 40 μM profilin (Rotty et al., 2015), and the inhibition of reconstituted propulsion of *Listeria* in the range of 10–50 μM profilin (Loisel et al., 1999) correlate with the inhibition of filament branching by profilin (Machesky et al., 1999; Rodal et al., 2003; Suarez et al., 2015). This effect required profilin's ability to bind actin, its binding to poly-L-proline being dispensable (Rotty et al., 2015; Suarez et al., 2015). However,

only binding of profilin to G-actin was considered in previous works.

We explored how profilin affects in vitro propulsion of N-WASP coated beads. Upon increasing profilin, the length of the actin tails decreased (Figure 5A) and branching density declined (Figures 5A and 5B). At 50 μM profilin, 60% of the beads moved only 2-fold slower than at 10 μM profilin (Figure S3A). Alexa 488-labeled Arp2/3 bound to N-WASP-coated beads identically at 3 or 50 μM profilin, testifying that only Arp2/3 incorporation in the tail is inhibited. Increasing the concentration of CP from 10 to 30 nM increased bead velocity by 22% at 20 μM profilin without restoring the original tail morphology. In summary, profilin inhibits filament branching by N-WASP-Arp2/3, corroborating recent reports (Rotty et al., 2015; Suarez et al., 2015).

Profilin also inhibited filament branching in spectrin-actin seeded polymerization assays with soluble VCA-Arp2/3, corroborating early (Machesky et al., 1999) and recent (Suarez et al., 2015) observations (Figure 5C). While 60 μM profilin slows down free barbed end growth by 2.2-fold, in the presence of Arp2/3 inhibition was much stronger than expected if only barbed end growth was inhibited (computed dashed curve in Figure 5C). The possibility that profilin competes with the WH2 domain of VCA for binding G-actin has been proposed (Suarez et al., 2015). Within this hypothesis, increasing VCA should balance out this effect. No reversal of the effect of 30 μM profilin was seen even by increasing the amount of VCA up to 10-fold (Figure S3B). Suarez et al. (2015) proposed that the direct competition between profilin and VCA for binding G-actin

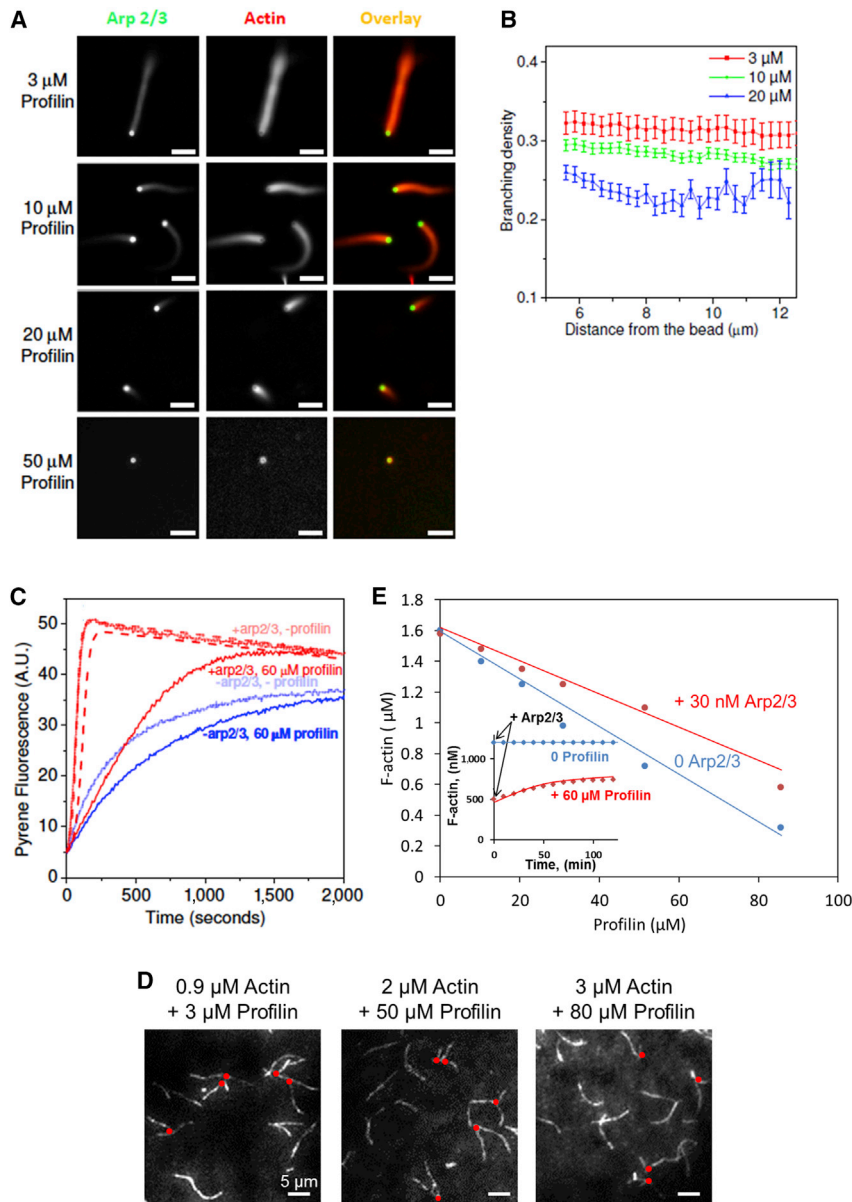


Figure 5. Profilin Inhibits Filament Branching by Arp2/3 Complex and Resulting Actin-Based Motility

(A) Double fluorescence (Alexa 594-actin and Alexa 488-Arp2/3) images of N-WASP-coated beads propelling in the reconstituted motility assay in the presence of profilin.

(B) Branching density ratio derived from integrated fluorescence intensity of Arp2/3 and actin along the comet tail.

(C) Effect of 60 μM profilin on barbed end growth initiated by 0.3 nM spectrin-actin seeds in the presence of 3 μM MgATP-G-actin and 0.16 μM VCA, in the absence and the presence of 46 nM Arp2/3 complex. Controls (no profilin) in dimmer colors. Dashed lines are calculated using a model (see Supplemental Experimental Procedures) in which filament branching is unaffected by profilin and filaments grow at the standard growth rate (dim red) and at a rate 55% lowered by profilin (bright red).

(D) Images of filaments branched with VCA and Arp2/3 complex at different concentrations of profilin after 1,000 s. Red dots, branch junctions.

(E) Destabilization of filaments by profilin is relieved by VCA-Arp2/3. Assembled F-actin in the presence of profilin and 50 nM VCA, with or without 30 nM Arp2/3. Inset: Increase in F-actin upon addition of Arp2/3 complex (30 nM) to F-actin pre-assembled with VCA and without (blue) or with (red) 60 μM profilin.

by the absence of profilin in large complexes in subcellular fractionation experiments (Kaiser et al., 1999). To distinguish between the two possibilities, we figured that if profilin simply inhibits Arp2/3, the destabilization of barbed ends by profilin at steady state should be unaffected by VCA-Arp2/3. In contrast, we find that the presence of VCA and Arp2/3 restores a higher level of F-actin (lower monomer concentration) in the presence of high amounts of profilin (Figure 5E). Thus, VCA and Arp2/3, like formin or VopF (Figures 4C and 4D), antagonize barbed end destabilization induced by profilin, supporting the view that filament branching by VCA-Arp2/3 takes place at barbed ends, at variance with the proposed side-branching model (Amann and Pollard, 2001a; Blanchoin et al., 2000).

accounted for the inhibition of branching competing directly with VCA for binding G-actin, but they actually found a 5-fold decrease in affinity of VCA for G-actin under conditions (1 μM actin, 20 μM profilin) where a 200-fold decrease was predicted by a mutually exclusive binding scheme. In conclusion, both our and Suarez et al.'s data exclude that profilin inhibits branching only by displacing G-actin from VCA. Profilin also inhibited filament branching in single-filament assays (Suarez et al., 2015) (Figure 5D).

Inhibition of Arp2/3-mediated dendritic meshworks, irrespective of the nature of the branching protein (WAVE, N-WASP, VCA, ActA), takes place in a concentration range (5–100 μM) at which profilin binds to filament barbed ends, suggesting that profilin inhibits filament branching at barbed ends (Pantaloni et al., 2000). However, profilin might also bind and inhibit Arp2/3 complex (Mullins et al., 1998), a possibility weakened

by the absence of profilin in large complexes in subcellular fractionation experiments (Kaiser et al., 1999). To distinguish between the two possibilities, we figured that if profilin simply inhibits Arp2/3, the destabilization of barbed ends by profilin at steady state should be unaffected by VCA-Arp2/3. In contrast, we find that the presence of VCA and Arp2/3 restores a higher level of F-actin (lower monomer concentration) in the presence of high amounts of profilin (Figure 5E). Thus, VCA and Arp2/3, like formin or VopF (Figures 4C and 4D), antagonize barbed end destabilization induced by profilin, supporting the view that filament branching by VCA-Arp2/3 takes place at barbed ends, at variance with the proposed side-branching model (Amann and Pollard, 2001a; Blanchoin et al., 2000).

Live TIRF Microscopy Analysis of Assembly of Branched Filaments Reveals that Barbed End Branching Prevails over Side Branching

The side-branching model was tempered by the conspicuous observation that branching was favored in the region that appeared close to the barbed end where ADP-Pi subunits were thought to facilitate side branching (Amann and Pollard, 2001b). However, no experimental evidence has established a role of bound nucleotide in branching. This hypothesis, which had been discarded previously (Blanchoin et al., 2000), was further disproved, as no massive increase in branching activity

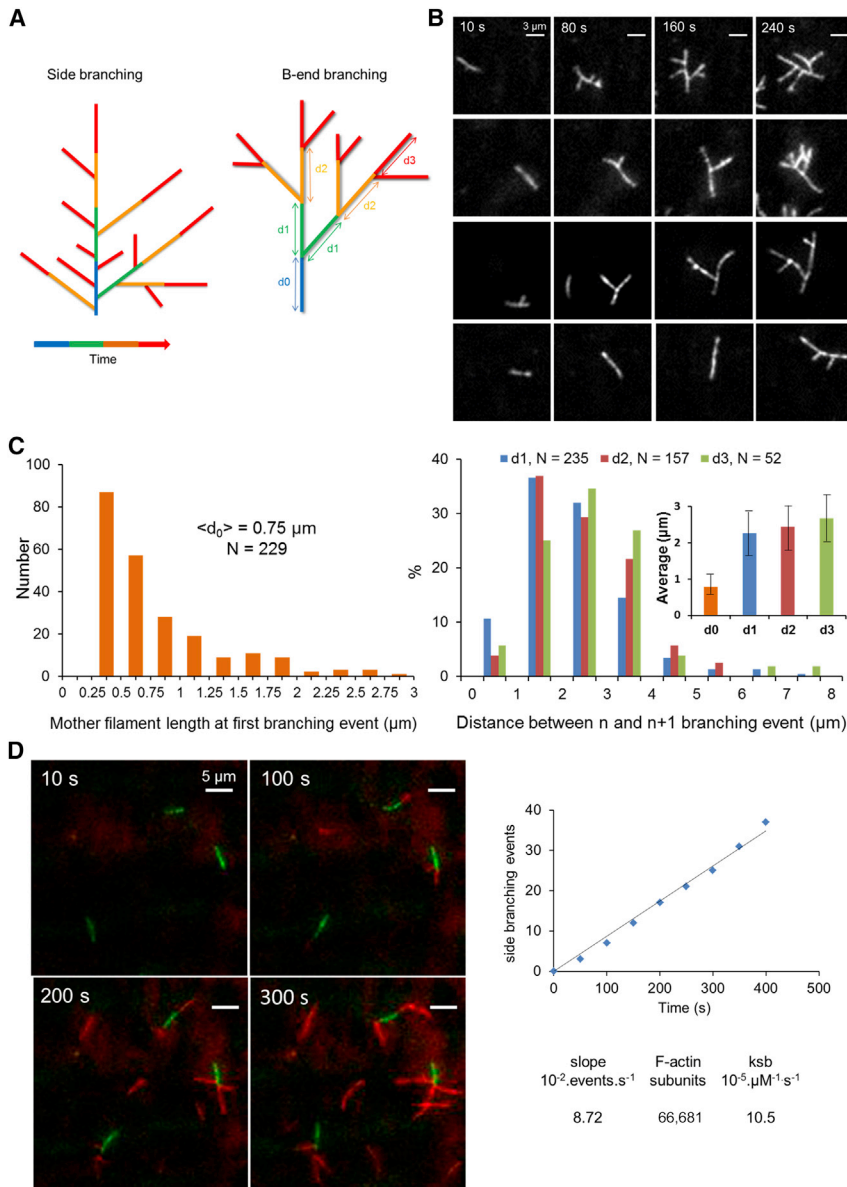


Figure 6. Filaments Branch upon Interaction of VCA-Arp2/3 Complex with Barbed Ends

(A) Sketch of morphologies of branched filaments initiated from a single nucleus and undergoing side branching only (left) or barbed end branching only (right). Rainbow color coding is used to indicate the time course of assembly.

(B) Time-lapse images of single filaments growing and branching with $0.9 \mu\text{M}$ actin (10% Alexa 488 labeled), 50 nM VCA, and 12.5 nM Arp2/3. See also [Movie S1](#).

(C) Distribution of branching distances d_0, d_1, d_2, d_3 between consecutive branching points. See text for details; Inset: average values of d_0, d_1, d_2, d_3 . See also [Movie S2](#).

(D) Left: Time-lapse images of side branching of filaments. Pre-assembled green filaments branching in the presence of red G-actin, VCA, and Arp2/3. Right: Frequency of side branching derived from the linear time dependence of side-branching events. See also [Movie S3](#).

constrained 2D geometry introduces biases and limits the rotational freedom of filaments (see [Supplemental Experimental Procedures](#)). To optimize the comparison of kinetic information derived from bulk solution and single-filament TIRF measurements of filament branching, we analyzed TIRF recordings of the spontaneous assembly of G-actin into non-anchored filaments branching and growing at a constant rate (see [Supplemental Experimental Procedures](#)). The following observations were made ([Figure 6B](#)). The first branching event B_0 occurs very early following nucleation, at a distance d_0 from the mother filament pointed end of less than $0.8 \mu\text{m}$, leading to a large number of symmetric V-shaped structures ([Figure 6B](#); [Movies S1](#) and [S2](#)). Notably, if branching occurred mainly from the side of filaments, the branching frequency derived from the value of d_0 would

was measured on F-ADP-Pi filaments ([Le Clairche et al., 2003](#)) or in the presence of BeF_3^- (here, [Figure S4](#)). However, several reports showed clear evidence of side branching off F-ADP filaments ([Smith et al., 2013](#); [Risca et al., 2012](#)), with a very low frequency of $3 \times 10^{-5} \mu\text{M}^{-1} \text{s}^{-1}$ ([Smith et al., 2013](#)). How two mechanisms of branching could co-exist is not understood from available data.

We reasoned that different morphologies of individual dendritic structures initiated from a single nucleus would be obtained within the “side-branching only” versus the “end-branching only” mechanisms. While end branching generates a dichotomic fractal morphology, side branching increases the branching density on older, longer exposed regions of the filaments, generating a more bushy morphology ([Figure 6A](#)).

Because filaments are helical, filament branching develops 3D arborescent structures. Observation of filament branching in a

generate such densely branched filaments that individual branches would be unresolvable in TIRF. In contrast, the next branching event B_1 on the mother filament takes place at a 3-fold larger distance d_1 from B_0 ([Figure 6C](#)). Moreover, the distances $d_1, d_2,$ and d_3 between consecutive branching points $B_0, B_1, B_2,$ and B_3 along the same mother filaments (see [Supplemental Experimental Procedures](#)) had the same value of $2.5 \pm 0.3 \mu\text{m}$ (925 ± 100 subunits) ($N = 250, 150,$ and 50 for $d_1, d_2,$ and d_3 respectively ([Figure 6C](#)).

Most branching events occurring in the plane of observation generated mother and daughter filaments of equal length ([Movies S1](#) and [S2](#)). Branching at an angle from the plane generated bright dots often leading to late emergence of already long filaments (see [Supplemental Experimental Procedures](#)). Rare side-branching events were identified (arrows in [Figure 6B](#) bottom panel and [Movie S1](#), right panel), so that the distance d_1

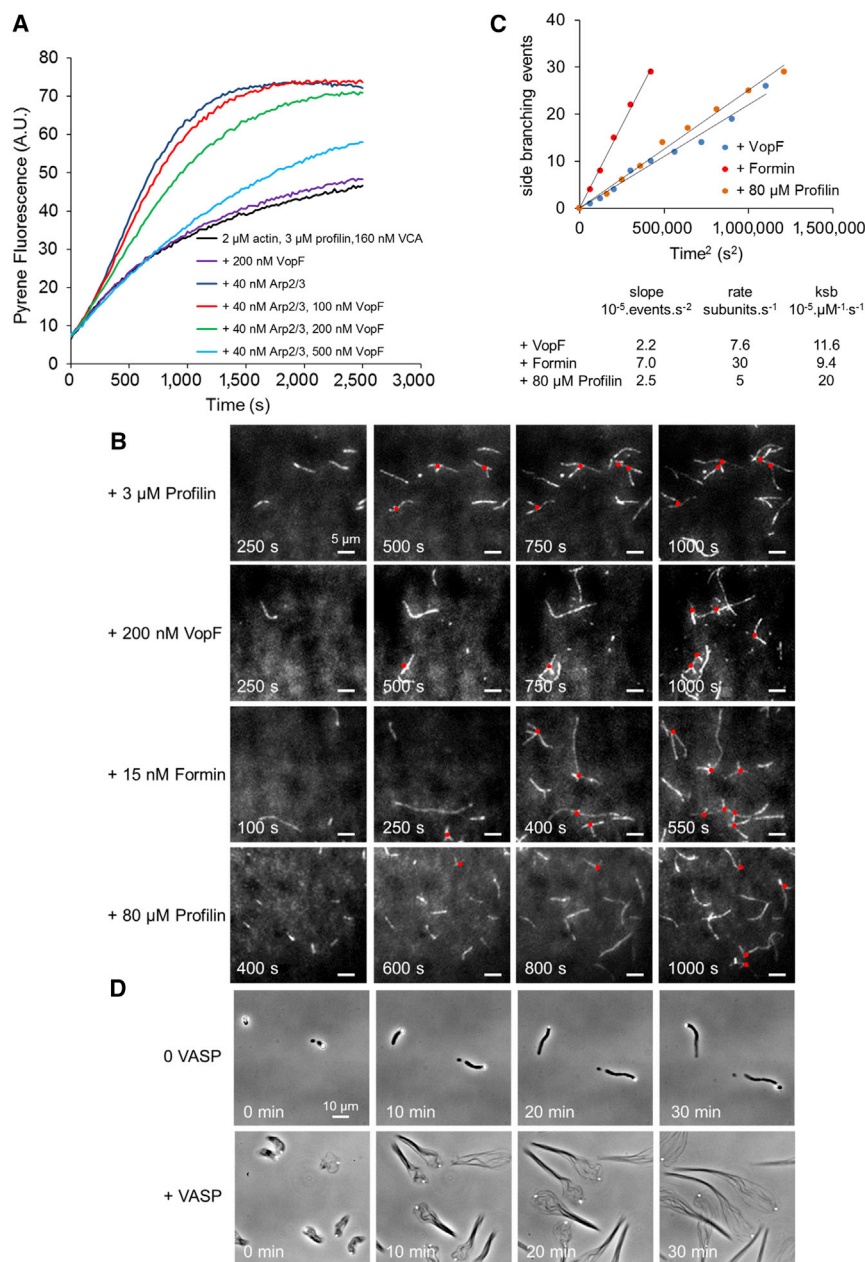


Figure 7. Barbed End Trackers Formin, VopF, and VASP and Destabilizer Profilin Compete with Filament Branching at Barbed Ends

(A) VopF inhibits filament branching by VCA and Arp2/3. Conditions as in Figure 5C. Spectrin-actin seeds 0.3 nM; actin (2 μM , 10% pyrenyl labeled), 3 μM profilin, 160 nM VCA, 40 nM Arp2/3 in the presence and the absence of VopF.

(B) Time-lapse images of filaments branching in the presence of 0.9 μM actin and 3 μM profilin, without or with 200 nM VopF, 15 nM FH1-FH2 mDia1, or 80 μM profilin. Red dots, branched junctions. See also Movie S4.

(C) Number of side-branching events as a function of t^2 in the presence of VopF, FH1-FH2, and profilin (data from B).

(D) Time-lapse phase contrast images of ActA-coated beads in a reconstituted motility assay (7 μM F-actin, 2 μM profilin, 100 nM Arp2/3, 3.5 μM ADF, and 200 nM gelsolin) in the absence (top) or the presence (bottom) of 100 nM VASP. See also Movie S5.

and assuming all the Arp2/3 (12.5 nM) to be in an active complex with VCA. The small value of d_0 compared with d_1 , d_2 , and d_3 suggests that barbed end branching of very short filaments prevents their loss by total disassembly.

The frequency of side branching was evaluated using a two-color fluorescence assay (Movie S3). Pre-assembled Alexa 488-actin filaments (green actin) were flushed in the chamber together with Alexa 594-G-actin (red actin), VCA, and Arp2/3. The frequency of side branching, k_{sb} , derived from the linear time dependence of the side branching of red filaments off the side of green filaments (Figure 6D and Supplemental Experimental Procedures, Equation 3) was $10.5 \times 10^{-5} \mu\text{M}^{-1} \text{s}^{-1}$, in satisfactory agreement with Smith et al. (2013) and with Figure 2D in Risca et al. (2012). Newly initiated red filaments branched in arbo-

rescent structures displaying the same morphology as in Figure 6B. Note that if only side branching was imposed to accommodate the data in Figure 6B, producing one branching event every 925 subunits on average, the frequency of side branching would have to be $1.08 \times 10^{-3} \mu\text{M}^{-1} \text{s}^{-1}$, that is, 10-fold higher than the actual value measured for k_{sb} .

appeared essentially conserved, within the SD, over 200 s following the appearance of B_1 . Note that monitoring of spontaneous assembly from G-actin facilitates the evidence for barbed end branching in the early steps of assembly when little F-actin has assembled. The probability of side branching increases as F-actin accumulates.

These data support the view that branching occurs mainly at barbed ends at a constant frequency as the filament is growing at constant rate. The contribution of side-branching events is too small to bias the evidence for the main process in the period of time investigated. The value of the frequency of barbed end branching, $k_{\text{bb}} = 0.9 \pm 0.1 \mu\text{M}^{-1} \text{s}^{-1}$ was derived from the measured filament growth rate (9 subunits/s) and the average distance between branching points (925 subunits),

rescent structures displaying the same morphology as in Figure 6B. Note that if only side branching was imposed to accommodate the data in Figure 6B, producing one branching event every 925 subunits on average, the frequency of side branching would have to be $1.08 \times 10^{-3} \mu\text{M}^{-1} \text{s}^{-1}$, that is, 10-fold higher than the actual value measured for k_{sb} .

The Arp2/3 Branching Machinery Competes with Proteins Tracking Barbed Ends

If filaments branch at barbed ends, proteins tracking or capping barbed ends should also compete with VCA-Arp2/3. This was actually observed. In a bulk solution assay, VopF inhibited filament branching, like profilin (Figure 7A). In TIRF assays, filaments elongating in the presence of barbed end-bound VopF

or FH1-FH2 of mDia1 failed to branch at barbed ends (Movie S4). The time course of F-actin assembly and the general pattern of branched filaments were dramatically different from the densely branched patterns observed in the absence of barbed end binding reagents. Only side branching occurred with the expected t^2 dependence due to the fact that the amount of F-actin exposed to side branching increases as filaments grow (Figures 7B and 7C and Equation 4, Supplemental Experimental Procedures). Finally, in the presence of 80 μM profilin, barbed end branching vanished and side branching supported the rare remaining branching events (Figures 7B and 7C). The same value of k_{sb} was derived from analysis of the samples containing either formin or VopF or profilin as in Figure 6D.

The barbed end polymerase VASP harbors “anti-capping” properties (Bear et al., 2002; Breitsprecher et al., 2008; Hansen and Mullins, 2010) using its WH2 domains, as VopF does. VASP was also suggested to be an “anti-branching” factor (Bear et al., 2002; Skoble et al., 2001). To get mechanistic insight into this behavior of VASP, we reconstituted actin-based propulsion of beads coated with the *Listeria* protein ActA, a functional homolog of N-WASP (Boujemaa-Paterski et al., 2001; Skoble et al., 2000). VASP binds FPPPP repeats in ActA (Niebuhr et al., 1997) and enhances *Listeria* motility by an unknown mechanism (Laurent et al., 1999; Loisel et al., 1999; Smith et al., 1996). ActA-coated beads propelled by sustained assembly of dense Arp2/3-branched actin tails. Addition of VASP in the medium promoted a dramatic change in the morphology of tails into long linear unbranched actin bundles strikingly similar to formin-induced tails (Benanti et al., 2015; Romero et al., 2004) and propulsion was 3-fold faster, indicating that VASP inhibits filament branching by ActA-Arp2/3 by tracking filament barbed ends (Figure 7D and Movie S5).

DISCUSSION

This work reveals a new face of profilin: Its interaction with actin filament barbed ends has profound effects on assembly dynamics, actin homeostasis, and resulting motility. Profilin promotes large fluctuations of filament length that evoke mild dynamic instability. Profilin stands as a major competitor of barbed end regulators such as CP, formins, WH2 domain proteins that track barbed ends, or the N-WASP-Arp2/3 filament branching machinery. Filament branching takes place mainly via association of WASP-Arp2/3 with terminal barbed end subunits, explaining the persistent polarity of the lamellipodial network. Profilin appears as a major coordinator of actin filament polarized growth in cell migration and developmental processes. Finally, our results clarify the still elusive aspects of “anti-capping” and “anti-branching” regulation of actin filament dynamics (Rotty et al., 2015).

Profilin Enhances Filament Barbed End Dynamics and Resulting Length Fluctuations

At the steady state of actin assembly, length fluctuations resulting from the different dynamics of ADP-Pi and ADP-actin are enhanced by profilin by a factor of ~ 5 –10. This mild dynamic instability affects the length distribution of filaments, by promoting total disassembly of short filaments. In our simulations, at an average growth rate of 1 subunit/s, more than 60% of nucleated

filaments disappear in a few minutes at 30 μM profilin due to length fluctuations, versus less than 30% in the absence of profilin.

Filament Assembly from Profilin-Actin Requires MgATP

While actin assembles well in filaments regardless of the nature of the bound nucleotide (ATP, ADP, or AMPPNP) and associated divalent metal ion (Mg^{2+} or Ca^{2+}), barbed end growth is observed only from profilin-MgATP-actin. Filament elongation from profilin-actin requires a drop in affinity of profilin following association of each profilin-actin to the barbed end. Profilin has a low affinity for terminal AMPPNP-F-actin, yet barbed end growth from profilin-AMPPNP-actin fails to proceed. Consistently, the isoenergetic square describing association of actin and profilin at barbed ends (Pantaloni and Carlier, 1993; Yarmola and Bubba, 2006) is satisfied in AMPPNP but not in MgATP. Perhaps cleavage of the γ -phosphoester bond of ATP on the terminal or penultimate subunit facilitates the structural change leading to dissociation of profilin from the barbed end.

Physiological Relevance of the Competition between Profilin and Barbed End Binding Proteins

CP is the major capping protein in cells. We find that in a concentration range of 10–100 μM profilin and 1–100 nM CP, competition between profilin and CP at barbed ends results in a lower amount of profilin-actin co-existing with F-actin and CP than in conventional views based on strong capping. In turn, the fraction of profilin in the free state is higher than expected. Do these results have physiological significance given the abundance and much higher affinity of CP than profilin for barbed ends? We believe they do, first because active CP is present at a few nanomolar, since 98% of the total amount of CP (1 μM) is maintained inactive in a high-affinity complex ($K_D = 7$ nM) with myotrophin/V1, present at 3 μM (Edwards et al., 2014; Fujiwara et al., 2014; Takeda et al., 2010). Second, in the range of 90–100% capped filaments, a drop of only a few percent promotes a massive change in the steady state of actin assembly (Walsh et al., 1984; Pernier et al., 2013). Estimates can be found for the amount of unassembled actin monomers in cells, but the concentrations of (polymerizable) profilin-actin and free profilin are not well known (Moseley and Goode, 2006; Sirotkin et al., 2010). Nevertheless, the measured rates of transient filament growth in motile processes match a concentration of a few micromolar profilin-actin, consistent with our proposed scenario in which profilin competes with CP at barbed ends. Competition may be expected as well between profilin and CPs such as Eps8, IQGAP1, or CapG, which bind barbed ends with affinities in the nanomolar range.

Kinetic and steady state F-actin measurements show that, at high concentration, profilin inhibits binding of formin or VopF to barbed ends. We confirm and build on observations of inhibition of filament branching by profilin made by Machesky et al. (1999), Rotty et al. (2015), and Suarez et al. (2015) to show that it is by binding to barbed ends that profilin inhibits filament branching by VCA, N-WASP, and ActA with Arp2/3 complex. The modest profilin-induced decrease in affinity of VCA for actin (Suarez et al., 2015) suggests that an active ternary complex forms between profilin, actin, and VCA, as reported for profilin, actin,

and β -thymosin/WH2 domains (Xue et al., 2014; Yarmola and Bubb, 2004). Inhibition of branching by binding of profilin to barbed ends is consistent with early observations (Cao et al., 1992) that, upon injection in cells, profilin in contrast with standard sequestering agents promotes selective disassembly of lamellipodial arrays. Our data support the view that injection of profilin abrogates barbed end branching at the leading edge, leading to loss of sustained formation of new filaments, loss of contacts between the membrane and the cytoskeleton, and subsequent pointed end disassembly of the array. Increasing profilin should also lower the extent of barbed end capping, which synergizes in slowing down migration. The facts that excess profilin slows down the motility of cancer cells (Roy and Jacobson, 2004) and abrogates a lamellipodial network in control cells while increasing F-actin in Arpc2^{-/-} cells (Rotty et al., 2015) are consistent with our data.

Our results support the following mechanistic view. In live cells, the concentration of polymerizable actin monomers results from the regulated cycles of assembly and disassembly of actin filaments (Carlier et al., 2015; Danuser et al., 2013; Xue and Robinson, 2013). The pools of capped, free, and tracker-bound barbed ends, free G-actin, profilin-actin, and free profilin are in a complex dynamic equilibrium. The pool of polymerizable monomeric actin is replenished, i.e., non-finite, and profilin orchestrates actin homeostasis. This view differs from the one in which several filament assembly machineries compete for a finite pool of actin monomers (Suarez et al., 2015).

Filament Branching Occurs Mainly via Association of VCA-Arp2/3 to Filament Barbed Ends

Evidence for barbed end branching by VCA-Arp2/3 is provided by the inhibition of branching by profilin and proteins that track filament barbed ends (formin, VopF, VASP), and by thermodynamic data showing that the destabilization of filament barbed ends by profilin is antagonized by VCA-Arp2/3. Consistently, capping of barbed ends is energetically more costly in the presence of VCA-Arp2/3 (Pantaloni et al., 2000) and gelsolin-capped filaments fail to stimulate branching (Figure 4 in Boujemaa-Pateriski et al., 2001). Other reported inhibitors of branching may also act at barbed ends. Our analysis of live imaging of filament branching clarify conflicting views regarding barbed end branching and side-branching mechanisms in providing estimates of the frequency of each process.

Analyses of filament branching were derived from fluorescence microscopy of fixed filaments, branched in the presence of phalloidin (Blanchoin et al., 2000) or from electron microscopy images of short branched filaments (Pantaloni et al., 2000). Often, filaments were tethered to the coverslip while being exposed to VCA and Arp2/3 (Amann and Pollard, 2001b; Risca et al., 2012; Smith et al., 2013). Most studies concentrated on analysis of side-branching events, favored when barbed ends were capped (Smith et al., 2013). Yet, in Figure 1D of Risca et al. (2012), 20% of surface-tethered red filaments display identifiable barbed end branching, consistent with a very low frequency k_{bb} of 0.06–0.11 $\mu\text{M}^{-1} \text{s}^{-1}$ (branching occurred at a distance of one-quarter of the length of green filaments assembled over 70–120 s).

In our experiments, in contrast, filaments are not tethered to the coverslip while being exposed to VCA and Arp2/3. The rota-

tional freedom of the nucleating and growing barbed ends is therefore closer to a situation in which filaments branch in 3D in solution, e.g., in pyrene-actin fluorescence assays of branched filament assembly. Hence, inhibition of branching by VopF or profilin is recorded both in bulk solution kinetics and in live fluorescence microscopy (compare Figures 7A and 7C, 5C and 7C, respectively), consistent with the view that barbed end branching is the predominant pathway. We find that immobilization of filaments by a streptavidin-biotin link appreciably impairs barbed end reactivity, slowing down both the growth rate and the branching frequency (Figure S5 and Movie S6).

Presumably, the same structural organization of the Arp2/3 subunits at the branched junction is built via either end branching or side branching. How can the same protein-protein contacts be eventually established via each pathway? One possibility is that the observed structural change of several actin subunits of the mother filament at the branch junction (Rouiller et al., 2008) is facilitated in barbed end branching. Another possibility is that the WH2 domain of VCA uses its ability to capture barbed ends (Co et al., 2007) in the branching reaction. The plasticity of the filament (Galkin et al., 2010) might allow side branching via insertion of the WH2 domain into the core of the filament, as WH2 domain proteins such as Spire or Cobl do (Carlier et al., 2013). The preferential side branching on the convex face of curved filaments (Risica et al., 2012) is suggestive of such a possibility. Further biochemical and structural experimentation and modeling are required to test this hypothesis.

In vivo, filament branching is catalyzed by small-size WASP proteins that localize at membranes in protrusive, compressive, or adhesive processes or at the surface of a pathogen where filament barbed ends abut. Barbed end branching ensures the persistence of polarized dendritic arrays and allows the growth of mother and daughter branches to equally contribute to production of force. Assuming a barbed end branching frequency of 1 $\mu\text{M}^{-1} \text{s}^{-1}$, and cellular concentrations of 1–5 μM profilin-actin and 0.1–0.2 μM Arp2/3, the branching distance would be between 0.1 and 0.5 μm , in satisfactory agreement with measurements in lamellipodia (Iwasa and Mullins, 2007). Our conclusions have profound implications regarding the molecular mechanism by which dendritic structures are formed in numerous processes dependent on WASP family proteins and Arp2/3 complex and on the associated physical mechanism of force production.

EXPERIMENTAL PROCEDURES

Proteins

Actin from rabbit muscle was isolated in G form, pyrenyl labeled on cysteine 374, and Alexa 488-, Alexa 594-, or biotin-labeled on lysines (Thermo Scientific). Arp2/3 was purified from ovine brain. Recombinant mouse profilin 1, N-WASP VCA, CP, gelsolin, VopF (Pernier et al., 2013), recombinant VASP (Laurent et al., 1999), ActA (Cicchetti et al., 1999), mDia1 FH1-FH2 (Romero et al., 2004), and biotinylated SNAP-tagged FH1-FH2 (Shekhar et al., 2015) were used.

Kinetic Measurements of Filament Barbed End Growth

Initial rates of filament barbed end growth or disassembly were monitored using the change in pyrenyl-actin fluorescence in a Safas Xenius spectrofluorimeter (Safas). For details see Supplemental Experimental Procedures.

Measurements of Assembled and Unassembled F-Actin at Steady State

F-Actin (labeled with 2% pyrenyl) was incubated overnight at 4°C in the dark in the presence of regulatory proteins. Fluorescence intensity was converted into F-actin amounts using standards. The concentration of unassembled actin reflected the thermodynamic stability of F-actin in the presence of effectors acting antagonistically at barbed ends. For details, see [Supplemental Experimental Procedures](#).

TIRF Microscopy of Single Filaments

Microfluidics-assisted TIRF microscopy was used to monitor the kinetics of filament growth or depolymerization using an Olympus IX71 microscope with a 60× oil objective and a Cascade II EMCCD (Photometrics) camera ([Jegou et al., 2011, 2013](#)). Filament assembly was initiated from spectrin-actin functionalized glass coverslips or from anchored formins ([Shekhar et al., 2015](#)). A standard open chamber TIRF method was used to monitor the kinetics of individual filament branching and growth in the presence of actin, VCA, and Arp2/3 complex. For details, see [Supplemental Experimental Procedures](#).

Numerical Simulations of Filament Elongation

Simulations were performed with a program written in C (free Bloodshed-DevC++ software) following a Gillespie algorithm. The length of individual filaments was computed over time for a population of at least 50 filaments for a given set of kinetic parameters. The same analysis of length fluctuations was performed on simulated and experimental data. See [Supplemental Experimental Procedures](#) for details.

Bead Motility Assay

Experiments were conducted as described previously ([Wiesner et al., 2003](#)), except for CP replacing gelsolin. For details, see [Supplemental Experimental Procedures](#).

SUPPLEMENTAL INFORMATION

Supplemental Information includes Supplemental Experimental Procedures, five figures, one table, and six movies and can be found with this article online at <http://dx.doi.org/10.1016/j.devcel.2015.12.024>.

AUTHOR CONTRIBUTIONS

M.F.C. designed the project, performed bulk solution experiments, and wrote the paper; J.P. performed and analyzed bulk solution and single-filament experiments; S.S. performed and analyzed single-filament and motility assays; A.J. performed and analyzed length fluctuations measurements; B.G. provided technical help and performed bulk solution measurements.

ACKNOWLEDGMENTS

We acknowledge support from ERC (advanced grant #249982) and EC FP7 #241548. We thank Emmanuele Helfer for [Movie S5](#). We thank Guillaume Romet-Lemonne for simulations ([Figures 1B, 1E, and 1F](#)), computed curves ([Figures 2B and 5C](#)), and data ([Figure 3A](#)).

Received: September 1, 2015

Revised: December 9, 2015

Accepted: December 22, 2015

Published: January 25, 2016

REFERENCES

Amann, K.J., and Pollard, T.D. (2001a). The Arp2/3 complex nucleates actin filament branches from the sides of pre-existing filaments. *Nat. Cell Biol.* **3**, 306–310.

Amann, K.J., and Pollard, T.D. (2001b). Direct real-time observation of actin filament branching mediated by Arp2/3 complex using total internal reflection fluorescence microscopy. *Proc. Natl. Acad. Sci. USA* **98**, 15009–15013.

Bear, J.E., Svitkina, T.M., Krause, M., Schafer, D.A., Loureiro, J.J., Strasser, G.A., Maly, I.V., Chaga, O.Y., Cooper, J.A., Borisy, G.G., et al. (2002). Antagonism between Ena/VASP proteins and actin filament capping regulates fibroblast motility. *Cell* **109**, 509–521.

Benanti, E.L., Nguyen, C.M., and Welch, M.D. (2015). Virulent Burkholderia species mimic host actin polymerases to drive actin-based motility. *Cell* **161**, 348–360.

Blanchoin, L., Amann, K.J., Higgs, H.N., Marchand, J.B., Kaiser, D.A., and Pollard, T.D. (2000). Direct observation of dendritic actin filament networks nucleated by Arp2/3 complex and WASP/Scar proteins. *Nature* **404**, 1007–1011.

Boujemaa-Paterski, R., Gouin, E., Hansen, G., Samarin, S., Le Clainche, C., Didry, D., Dehoux, P., Cossart, P., Kocks, C., Carlier, M.F., et al. (2001). Listeria protein ActA mimics WASP family proteins: it activates filament barbed end branching by Arp2/3 complex. *Biochemistry* **40**, 11390–11404.

Breitsprecher, D., Kieseewetter, A.K., Linkner, J., Urbanke, C., Resch, G.P., Small, J.V., and Faix, J. (2008). Clustering of VASP actively drives processive, WH2 domain-mediated actin filament elongation. *EMBO J.* **27**, 2943–2954.

Bubb, M.R., Yarmola, E.G., Gibson, B.G., and Southwick, F.S. (2003). Depolymerization of actin filaments by profilin. Effects of profilin on capping protein function. *J. Biol. Chem.* **278**, 24629–24635.

Cao, L.G., Babcock, G.G., Rubenstein, P.A., and Wang, Y.L. (1992). Effects of profilin and profilactin on actin structure and function in living cells. *J. Cell Biol.* **117**, 1023–1029.

Carlier, M.F., and Pantaloni, D. (1997). Control of actin dynamics in cell motility. *J. Mol. Biol.* **269**, 459–467.

Carlier, M.F., Pantaloni, D., and Korn, E.D. (1984). Evidence for an ATP cap at the ends of actin filaments and its regulation of the F-actin steady state. *J. Biol. Chem.* **259**, 9983–9986.

Carlier, M.F., Pernier, J., and Avvaru, B.S. (2013). Control of actin filament dynamics at barbed ends by WH2 domains: from capping to permissive and processive assembly. *Cytoskeleton* **70**, 540–549.

Carlier, M.F., Pernier, J., Montaville, P., Shekhar, S., and Kuhn, S. (2015). Control of polarized assembly of actin filaments in cell motility. *Cell Mol. Life Sci.* **72**, 3051–3067.

Cicchetti, G., Maurer, P., Wagener, P., and Kocks, C. (1999). Actin and phosphoinositide binding by the ActA protein of the bacterial pathogen *Listeria monocytogenes*. *J. Biol. Chem.* **274**, 33616–33626.

Co, C., Wong, D.T., Gierke, S., Chang, V., and Taunton, J. (2007). Mechanism of actin network attachment to moving membranes: barbed end capture by N-WASP WH2 domains. *Cell* **128**, 901–913.

Courtemanche, N., and Pollard, T.D. (2013). Interaction of profilin with the barbed end of actin filaments. *Biochemistry* **52**, 6456–6466.

Danuser, G., Allard, J., and Mogilner, A. (2013). Mathematical modeling of eukaryotic cell migration: insights beyond experiments. *Annu. Rev. Cell Dev. Biol.* **29**, 501–528.

dos Remedios, C.G., Chhabra, D., Kekic, M., Dedova, I.V., Tsubakihara, M., Berry, D.A., and Nosworthy, N.J. (2003). Actin binding proteins: regulation of cytoskeletal microfilaments. *Physiol. Rev.* **83**, 433–473.

Edwards, M., Zwolak, A., Schafer, D.A., Sept, D., Dominguez, R., and Cooper, J.A. (2014). Capping protein regulators fine-tune actin assembly dynamics. *Nat. Rev. Mol. Cell Biol.* **15**, 677–689.

Fujiwara, I., Takahashi, S., Tadakuma, H., Funatsu, T., and Ishiwata, S. (2002). Microscopic analysis of polymerization dynamics with individual actin filaments. *Nat. Cell Biol.* **4**, 666–673.

Fujiwara, I., Remmert, K., Piszczek, G., and Hammer, J.A. (2014). Capping protein regulatory cycle driven by CARMIL and V-1 may promote actin network assembly at protruding edges. *Proc. Natl. Acad. Sci. USA* **111**, E1970–E1979.

Galkin, V.E., Orlova, A., Schroder, G.F., and Egelman, E.H. (2010). Structural polymorphism in F-actin. *Nat. Struct. Mol. Biol.* **17**, 1318–1323.

Goode, B.L., and Eck, M.J. (2007). Mechanism and function of formins in the control of actin assembly. *Annu. Rev. Biochem.* **76**, 593–627.

- Hansen, S.D., and Mullins, R.D. (2010). VASP is a processive actin polymerase that requires monomeric actin for barbed end association. *J. Cell Biol.* *191*, 571–584.
- Higgs, H.N. (2005). Formin proteins: a domain-based approach. *Trends Biochem. Sci.* *30*, 342–353.
- Hill, T.L. (1986). Theoretical study of a model for the ATP cap at the end of an actin filament. *Biophys. J.* *49*, 981–986.
- Hug, C., Jay, P.Y., Reddy, I., McNally, J.G., Bridgman, P.C., Elson, E.L., and Cooper, J.A. (1995). Capping protein levels influence actin assembly and cell motility in dictyostelium. *Cell* *81*, 591–600.
- Iwasa, J.H., and Mullins, R.D. (2007). Spatial and temporal relationships between actin-filament nucleation, capping, and disassembly. *Curr. Biol.* *17*, 395–406.
- Jegou, A., Niedermayer, T., Orban, J., Didry, D., Lipowsky, R., Carlier, M.F., and Romet-Lemonne, G. (2011). Individual actin filaments in a microfluidic flow reveal the mechanism of ATP hydrolysis and give insight into the properties of profilin. *PLoS Biol.* *9*, e1001161.
- Jegou, A., Carlier, M.F., and Romet-Lemonne, G. (2013). Formin mDia1 senses and generates mechanical forces on actin filaments. *Nat. Commun.* *4*, 1883.
- Joy, M.E., Vollmer, L.L., Hulkower, K., Stern, A.M., Peterson, C.K., Boltz, R.C., Roy, P., and Vogt, A. (2014). A high-content, multiplexed screen in human breast cancer cells identifies profilin-1 inducers with anti-migratory activities. *PLoS One* *9*, e88350.
- Kaiser, D.A., Vinson, V.K., Murphy, D.B., and Pollard, T.D. (1999). Profilin is predominantly associated with monomeric actin in *Acanthamoeba*. *J. Cell Sci.* *112*, 3779–3790.
- Kinosian, H.J., Selden, L.A., Gershman, L.C., and Estes, J.E. (2002). Actin filament barbed end elongation with nonmuscle MgATP-actin and MgADP-actin in the presence of profilin. *Biochemistry* *41*, 6734–6743.
- Kovar, D.R., Kuhn, J.R., Tichy, A.L., and Pollard, T.D. (2003). The fission yeast cytokinesis formin Cdc12p is a barbed end actin filament capping protein gated by profilin. *J. Cell Biol.* *161*, 875–887.
- Kovar, D.R., Harris, E.S., Mahaffy, R., Higgs, H.N., and Pollard, T.D. (2006). Control of the assembly of ATP- and ADP-actin by formins and profilin. *Cell* *124*, 423–435.
- Kuhn, J.R., and Pollard, T.D. (2005). Real-time measurements of actin filament polymerization by total internal reflection fluorescence microscopy. *Biophys. J.* *88*, 1387–1402.
- Laurent, V., Loisel, T.P., Harbeck, B., Wehman, A., Grobe, L., Jockusch, B.M., Wehland, J., Gertler, F.B., and Carlier, M.F. (1999). Role of proteins of the Ena/VASP family in actin-based motility of *Listeria monocytogenes*. *J. Cell Biol.* *144*, 1245–1258.
- Le Clainche, C., Pantaloni, D., and Carlier, M.F. (2003). ATP hydrolysis on actin-related protein 2/3 complex causes debranching of dendritic actin arrays. *Proc. Natl. Acad. Sci. USA* *100*, 6337–6342.
- Loisel, T.P., Boujemaa, R., Pantaloni, D., and Carlier, M.F. (1999). Reconstitution of actin-based motility of *Listeria* and *Shigella* using pure proteins. *Nature* *401*, 613–616.
- Lorente, G., Syriani, E., and Morales, M. (2014). Actin filaments at the leading edge of cancer cells are characterized by a high mobile fraction and turnover regulation by profilin I. *PLoS One* *9*, e85817.
- Machesky, L.M., Mullins, R.D., Higgs, H.N., Kaiser, D.A., Blanchoin, L., May, R.C., Hall, M.E., and Pollard, T.D. (1999). Scar, a WASp-related protein, activates nucleation of actin filaments by the Arp2/3 complex. *Proc. Natl. Acad. Sci. USA* *96*, 3739–3744.
- Moseley, J.B., and Goode, B.L. (2006). The yeast actin cytoskeleton: from cellular function to biochemical mechanism. *Microbiol. Mol. Biol. Rev.* *70*, 605–645.
- Mullins, R.D., Kelleher, J.F., Xu, J., and Pollard, T.D. (1998). Arp2/3 complex from *Acanthamoeba* binds profilin and cross-links actin filaments. *Mol. Biol. Cell* *9*, 841–852.
- Niebuhr, K., Ebel, F., Frank, R., Reinhard, M., Domann, E., Carl, U.D., Walter, U., Gertler, F.B., Wehland, J., and Chakraborty, T. (1997). A novel proline-rich motif present in ActA of *Listeria monocytogenes* and cytoskeletal proteins is the ligand for the EVH1 domain, a protein module present in the Ena/VASP family. *EMBO J.* *16*, 5433–5444.
- Pantaloni, D., and Carlier, M.F. (1993). How profilin promotes actin filament assembly in the presence of thymosin beta 4. *Cell* *75*, 1007–1014.
- Pantaloni, D., Boujemaa, R., Didry, D., Gounon, P., and Carlier, M.F. (2000). The Arp2/3 complex branches filament barbed ends: functional antagonism with capping proteins. *Nat. Cell Biol.* *2*, 385–391.
- Pernier, J., Orban, J., Avvaru, B.S., Jegou, A., Romet-Lemonne, G., Guichard, B., and Carlier, M.F. (2013). Dimeric WH2 domains in *Vibrio* VopF promote actin filament barbed-end uncapping and assisted elongation. *Nat. Struct. Mol. Biol.* *20*, 1069–1076.
- Pollard, T.D., and Cooper, J.A. (1984). Quantitative analysis of the effect of *Acanthamoeba* profilin on actin filament nucleation and elongation. *Biochemistry* *23*, 6631–6641.
- Ranjith, P., Lacoste, D., Mallick, K., and Joanny, J.F. (2009). Nonequilibrium self-assembly of a filament coupled to ATP/GTP hydrolysis. *Biophys. J.* *96*, 2146–2159.
- Risca, V.I., Wang, E.B., Chaudhuri, O., Chia, J.J., Geissler, P.L., and Fletcher, D.A. (2012). Actin filament curvature biases branching direction. *Proc. Natl. Acad. Sci. USA* *109*, 2913–2918.
- Rodal, A.A., Manning, A.L., Goode, B.L., and Drubin, D.G. (2003). Negative regulation of yeast WASp by two SH3 domain-containing proteins. *Curr. Biol.* *13*, 1000–1008.
- Romero, S., Le Clainche, C., Didry, D., Egile, C., Pantaloni, D., and Carlier, M.F. (2004). Formin is a processive motor that requires profilin to accelerate actin assembly and associated ATP hydrolysis. *Cell* *119*, 419–429.
- Rotty, J.D., Wu, C., Haynes, E.M., Suarez, C., Winkelman, J.D., Johnson, H.E., Haugh, J.M., Kovar, D.R., and Bear, J.E. (2015). Profilin-1 serves as a gatekeeper for actin assembly by Arp2/3-dependent and -independent pathways. *Dev. Cell* *32*, 54–67.
- Rouiller, I., Xu, X.P., Amann, K.J., Egile, C., Nickell, S., Nicastro, D., Li, R., Pollard, T.D., Volkman, N., and Hanein, D. (2008). The structural basis of actin filament branching by the Arp2/3 complex. *J. Cell Biol.* *180*, 887–895.
- Roy, P., and Jacobson, K. (2004). Overexpression of profilin reduces the migration of invasive breast cancer cells. *Cell Motil. Cytoskeleton* *57*, 84–95.
- Scott, B.J., Neidt, E.M., and Kovar, D.R. (2011). The functionally distinct fission yeast formins have specific actin-assembly properties. *Mol. Biol. Cell* *22*, 3826–3839.
- Shekhar, S., Kerleau, M., Kuhn, S., Pernier, J., Romet-Lemonne, G., Jegou, A., and Carlier, M.F. (2015). Formin and capping protein together embrace the actin filament in a menage a trois. *Nat. Commun.* *6*, 8730.
- Sirotkin, V., Berro, J., Macmillan, K., Zhao, L., and Pollard, T.D. (2010). Quantitative analysis of the mechanism of endocytic actin patch assembly and disassembly in fission yeast. *Mol. Biol. Cell* *21*, 2894–2904.
- Skoble, J., Portnoy, D.A., and Welch, M.D. (2000). Three regions within ActA promote Arp2/3 complex-mediated actin nucleation and *Listeria* motility. *J. Cell Biol.* *150*, 527–538.
- Skoble, J., Auerbuch, V., Goley, E.D., Welch, M.D., and Portnoy, D.A. (2001). Pivotal role of VASP in Arp2/3 complex-mediated actin nucleation, actin branch-formation, and *Listeria* motility. *J. Cell Biol.* *155*, 89–100.
- Smith, G.A., Theriot, J.A., and Portnoy, D.A. (1996). The tandem repeat domain in the *Listeria* motility protein ActA controls the rate of actin-based motility, the percentage of moving bacteria, and the localization of vasodilator-stimulated phosphoprotein and profilin. *J. Cell Biol.* *135*, 647–660.
- Smith, B.A., Daugherty-Clarke, K., Goode, B.L., and Gelles, J. (2013). Pathway of actin filament branch formation by Arp2/3 complex revealed by single-molecule imaging. *Proc. Natl. Acad. Sci. USA* *110*, 1285–1290.
- Stukalin, E.B., and Kolomeisky, A.B. (2006). ATP hydrolysis stimulates large length fluctuations in single actin filaments. *Biophys. J.* *90*, 2673–2685.

- Suarez, C., Carroll, R.T., Burke, T.A., Christensen, J.R., Bestul, A.J., Sees, J.A., James, M.L., Sirotkin, V., and Kovar, D.R. (2015). Profilin regulates F-actin network homeostasis by favoring formin over Arp2/3 complex. *Dev. Cell* **32**, 43–53.
- Takeda, S., Minakata, S., Koike, R., Kawahata, I., Narita, A., Kitazawa, M., Ota, M., Yamakuni, T., Maeda, Y., and Nitani, Y. (2010). Two distinct mechanisms for actin capping protein regulation—steric and allosteric inhibition. *PLoS Biol.* **8**, e1000416.
- Vavylonis, D., Yang, Q., and O’Shaughnessy, B. (2005). Actin polymerization kinetics, cap structure, and fluctuations. *Proc. Natl. Acad. Sci. USA* **102**, 8543–8548.
- Walsh, T.P., Weber, A., Higgins, J., Bonder, E.M., and Mooseker, M.S. (1984). Effect of villin on the kinetics of actin polymerization. *Biochemistry* **23**, 2613–2621.
- Wear, M.A., Yamashita, A., Kim, K., Maeda, Y., and Cooper, J.A. (2003). How capping protein binds the barbed end of the actin filament. *Curr. Biol.* **13**, 1531–1537.
- Wiesner, S., Helfer, E., Didry, D., Ducouret, G., Lafuma, F., Carlier, M.-F., and Pantaloni, D. (2003). A biomimetic motility assay provides insight into the mechanism of actin-based motility. *J. Cell Biol.* **160**, 387–398.
- Witke, W., Sutherland, J.D., Sharpe, A., Arai, M., and Kwiatkowski, D.J. (2001). Profilin I is essential for cell survival and cell division in early mouse development. *Proc. Natl. Acad. Sci. USA* **98**, 3832–3836.
- Xue, B., and Robinson, R.C. (2013). Guardians of the actin monomer. *Eur. J. Cell Biol.* **92**, 316–332.
- Xue, B., Leyrat, C., Grimes, J.M., and Robinson, R.C. (2014). Structural basis of thymosin-beta4/profilin exchange leading to actin filament polymerization. *Proc. Natl. Acad. Sci. USA* **111**, E4596–E4605.
- Yarmola, E.G., and Bubba, M.R. (2004). Effects of profilin and thymosin beta4 on the critical concentration of actin demonstrated in vitro and in cell extracts with a novel direct assay. *J. Biol. Chem.* **279**, 33519–33527.
- Yarmola, E.G., and Bubba, M.R. (2006). Profilin: emerging concepts and lingering misconceptions. *Trends. Biochem. Sci.* **31**, 197–205.